ELSEVIER

Agricultural and Forest Meteorology 93 (1999) 243–258

AGRICULTURAL AND FOREST METEOROLOGY

Wind and remnant tree sway in forest cutblocks. II. Relating measured tree sway to wind statistics

Thomas K. Flesch*, John D. Wilson

Department of Earth and Atmospheric Sciences, University of Alberta, Edmonton Alb., Canada T6G 2E3

Received 18 March 1998; accepted 15 September 1998

Abstract

New silvicultural designs use unharvested forest strips to provide wind shelter in harvest cutblocks, and reduce windthrow of remnant trees. In this study we attempted to quantify wind shelter in terms of tree sway. We investigated the relationship between wind statistics and tree sway in two cutblocks in northern Alberta, Canada: a narrow cutblock (1.7 canopy heights in width, $X_c = 1.7$ h), and a wide cutblock ($X_c = 6.1$ h). We focused on the case of winds oriented across the cutblock width. The instantaneous across- and along-cutblock wind 'forces' acting on an understory white spruce (*Picea glauca*) were considered as proportional to $u|u|$ and $v|v|$, where u and v are the across- and along-cutblock wind velocities at height $z = 0.4$ h. A simple mass–spring–damper displacement model, calibrated to tree sway measurements, was used to diagnose the sway response of a 'characteristic' remnant spruce (damping coefficient $\zeta = 0.11$, natural frequency $\omega_n = 0.4$ Hz). We determined that in the cutblocks this characteristic tree: (i) had a small average angular displacement $\langle\theta\rangle$ relative to its maximum displacement θ_{max}; (ii) exhibited 'resonant sway,' where the interaction of tree dynamics and turbulence increased sway by 10–35% over that expected if displacement was proportional to the instantaneous wind force; and (iii) had sway statistics which correlated well with the standard deviation of wind force $\sigma_{u|u|}$. Modelled tree sway was used to infer the degree of windthrow protection in the sheltered cutblocks. Our approach was to predict a threshold average wind velocity in the open (U_w, essentially a weather station windspeed) which correlates with the occurrence of windthrow of remnant spruce in the cutblock. Our *assumption* was that an average velocity of 10 m s^{-1} causes windthrow of unprotected trees in the open. Larger windspeeds (U_w) are needed to cause windthrow in the cutblocks. In the wide cutblock U_w varied from 13 m s^{-1} near the downwind forest edge to 25 m s^{-1} near the upwind edge. In the narrow cutblock U_w varied from 19 m s^{-1} at the downwind edge to 30 m s^{-1} at the upwind edge. The most effective wind shelter, as given by the highest U_w, was within three tree heights of the upwind forest. In designing harvest cutblocks to reduce windthrow, we suggest that cutblocks not exceed three tree heights in width.

Keywords: Windthrow; Windbreaks; Tree sway; Forest management

1. Introduction

In the aspen (*Populus tremuloides*) and white spruce (*Picea glauca*) mixedwoods of Canada, foresters are investigating aspen harvest techniques that preserve the commercially and ecologically valuable spruce understory. An obstacle to this 'two-stage' harvest is the susceptibility of the remnant spruce to windthrow (uprooting) after aspen removal. One approach to this problem, discussed in the preceding paper (Flesch and Wilson, 1999), is a shelterwood harvest system. In a shelterwood design (Fig. 1) the aspen is

*Corresponding author. E-mail: thomas.flesch@ualberta.ca

0168-1923/99/$ – see front matter
PII: S0168-1923(98)00113-0

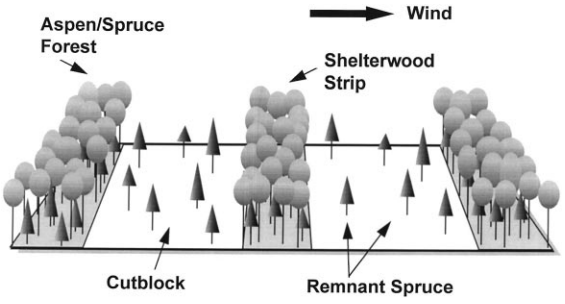

Fig. 1. Idealised view of a shelterwood harvest system. Cutblocks are created by selectively harvesting the mature aspen overstory, leaving the spruce understory intact. Forest strips (shelterwood) separate the cutblocks, providing wind shelter.

harvested in a series of narrow cutblocks that are separated by unharvested forest strips (shelterwood). The forest strips provide a degree of wind shelter for the remnant spruce.

Flesch and Wilson (1999) described the wind statistics in two shelterwood cutblocks when the wind was oriented across the cutblocks' width. In the cutblock immediately downwind of the forest edge was a quiet zone, where the average across-cutblock wind velocity (U) and the turbulent kinetic energy (TKE) were reduced relative to the levels found in a nearby large reference clearing. This 'quiet' zone was concentrated within three forest canopy heights (h) of the upwind forest edge (at the measurement height of $z = 0.4$ h). Further downwind was a 'wake' zone, where the TKE was at, or slightly above, the level in the reference clearing.

Although these observations confirm the existence of wind shelter within cutblocks, the extent and effectiveness of this shelter in terms of windthrow reduction are indefinite without consideration of the nature of the vulnerable trees themselves. Because the strain on the tree/soil complex results from the interaction of wind forces and tree mechanical properties (as well as soil properties), we cannot assume that wind statistics alone fully determine tree behaviour, and therefore windthrow occurrence. The work of Holbo et al. (1980), Mayer (1987), Gardiner (1994), and others has shown that trees behave as vibrating systems. In the terminology of systems theory, trees can act as amplifiers, with wind energy near their natural frequency(s) (ω_n) preferentially transferred into tree sway and strain on the tree/soil complex, and as low-pass filters, with high frequency wind energy adding little to the strain. If the turbulent wind force fluctuates at frequencies near ω_n, windthrow may occur at wind forces below the critical static load required to uproot a tree (Oliver and Mayhead, 1974; Blackburn et al., 1988). Understanding tree response therefore requires consideration of not only simple wind statistics, such as average and standard deviation of the wind, but also of the frequency characteristics of turbulence and dynamical characteristics of the tree.

In this study we attempt to quantify cutblock wind shelter in terms of the magnitude of tree sway. Our assumption is that greater sway means greater strain on the tree/soil complex, and a greater likelihood of windthrow. Our analysis is based on a set of tree sway measurements, from which we formulated a simple mathematical model of tree displacement for a 'characteristic' remnant spruce. This model is combined with observations of wind velocity in harvest cutblocks to diagnose spatial variation in tree sway. Our analysis relies on spectral methods, similar to those employed by Holbo et al. (1980) and Mayer (1987). We consider only the case where the ambient wind direction was across the width of the cutblocks.

2. Field measurements

2.1. Study site

Field measurements were made at the site of silvicultural trials at Hotchkiss River, near Manning, Alberta, Canada. The area is classified as boreal mixedwoods, having a predominantly aspen overstory of 20–25 m in height, with a significant white spruce understory averaging 10 m in height. The site is on a gently rolling landscape. During the initial harvest, aspen and mature spruce were removed from long rectangular cutblocks. These varied in length from approximately 500 to 1000 m, and ranged in width from approximately 40 to 150 m. The cutblocks were oriented perpendicular to the direction of the expected maximum winds (westerly). Remnant spruce density in the cutblocks varied according to the density of the original understory. The forest canopy height (h) was 23 m.

Two cutblocks were studied: a wide cutblock with width $X_c = 140$ m (X_c/h = 6.1) and a length of 500 m,

and a narrow cutblock with $X_c = 40$ m ($X_c/h = 1.7$) and length of 700 m. These cutblocks were each one of a periodic series, separated by forest strips of roughly the same width as the cutblocks (the layout of these cutblocks are illustrated in Fig. 2(a, b) in Flesch and Wilson, 1999). We defined x as the across-cutblock coordinate (very nearly east–west), y as the along-cutblock coordinate (we expect flow properties to be roughly independent of y when winds were westerly), and z as the vertical coordinate. The coordinate x was set to zero at the upwind (west) edge of the instrumented cutblocks.

2.2. Wind measurements

Wind velocity time series were measured using three-dimensional propeller anemometers (R.M. Young, Gill UVW anemometer). Anemometers were placed at a height $z = 9$ m ($z/h = 0.4$) in transects across the two study cutblocks (the wide cutblock in 1994 and 1995, and the wide cutblock in 1996 and 1997). Measurements were made at five locations across the wide cutblock (at $x/h = -0.8$, 1.0, 3.2, 5.4, and 7.2), and five locations across the narrow cutblock (at $X/h = -1.2$, 0.2, 0.7, 1.1, and 1.5). We selected sites where the residual spruce density was low, and cut down the few trees that might have created wind anomalies along the transect. Measurements were made during periods of strong winds directly across the cutblock (along the x direction, $\pm$ 30 deg). The sampling periods lasted either 15 min (wide cutblock) or 30 min (narrow cutblock), with a sampling frequency of 5 Hz. At each location there were either five or six observation periods (excepting observations at $x/h = -1.2$ and 0.7 in the narrow cutblock, where only two periods were used). The measurement periods are listed in Table 1. We used u, v, w to denote the instantaneous across-cutblock velocity (x direction), along-cutblock velocity (y direction), and the vertical velocity, respectively.

During our experiment, average wind speed (S_{clr}) and direction were measured in a large 'reference' clearing 5 km from the study cutblocks. A cup anemometer (Met-One, model 013A) and wind vane were placed at $z = 9$ m approximately 20 h downwind from the forest edge (for the wind direction studied here). The clearing extended a further 20 h downwind of the tower. Throughout this work we will use S_{clr} as a velocity scale to normalise our in-cutblock data, to permit an assessment of the windiness of the cutblock *relative* to an essentially open region. We will also use S_{clr} and wind direction to derive a reference velocity in

Table 1
Measurement periods used in the study

No.	Cutblock width	Date	Time	S_{clr} (m s^{-1})	Wind direction (0 is across the cutblock)	Gill UVW locations	Tree sway measurement locations
W-1	6.1 h	27 Oct. 1994	1345–1400	6.41	3 deg	$x/h = 1.0, 3.2, 5.4$	$x/h = 3.1, 3.3$
W-2	6.1 h	28 Oct. 1994	1015–1030	4.85	4 deg	$x/h = 1.0, 3.2, 5.4$	$x/h = 3.1, 3.3$
W-3	6.1 h	28 Oct. 1994	1145–1200	4.97	16 deg	$x/h = 1.0, 3.2, 5.4$	$x/h = 3.1, 3.3$
W-4	6.1 h	28 Oct. 1994	1200–1215	5.86	25 deg	$x/h = 0, 3.2, 5.4$	$x/h = 3.1, 3.3$
W-5	6.1 h	4 Nov. 1994	1100–1115	6.21	3 deg	$x/h = 1.0, 3.2, 5.4$	$x/h = 3.1, 3.3$
W-6	6.1 h	18 Nov. 1994	1615–1630	5.21	16 deg	$x/h = 1.0, 3.2, 5.4$	$x/h = 3.1, 3.3$
W-7	6.1 h	26 Oct. 1995	1145–1200	3.69	10 deg	$x/h = -0.8, 3.2, 7.2$	$x/h = 3.0, 3.2$
W-8	6.1 h	26 Oct. 1995	1200–1215	3.70	24 deg	$x/h = -0.8, 3.2, 7.2$	$x/h = 3.0, 3.2$
W-9	6.1 h	26 Oct. 1995	1545–1600	4.21	−7 deg	$x/h = -0.8, 3.2, 7.2$	$x/h = 3.0, 3.2$
W-10	6.1 h	26 Oct. 1995	1615–1630	3.47	−14 deg	$x/h = -0.8, 3.2, 7.2$	$x/h = 3.0, 3.2$
W-12	6.1 h	26 Oct. 1995	1730–1745	4.39	−15 deg	$x/h = -0.8, 3.2, 7.2$	$x/h = 3.0, 3.2$
N-1	1.7 h	7 Oct. 1996	1100–1130	4.71	4 deg	$x/h = 0.2, 1.1, 1.5$	$x/h = 0.2, 1.5$
N-2	1.7 h	11 Oct. 1996	900–930	7.50	−13 deg	$x/h = 0.2, 1.1, 1.5$	$x/h = 0.2, 1.5$
N-3	1.7 h	11 Oct. 1996	1000–1030	7.06	−10 deg	$x/h = 0.2, 1.1, 1.5$	$x/h = 0.2, 1.5$
N-4	1.7 h	11 Oct. 1996	1200–1230	6.89	−3 deg	$x/h = 0.2, 1.1, 1.5$	$x/h = 0.2, 1.5$
N-5	1.7 h	11 Oct. 1996	1400–1430	7.82	0 deg	$x/h = 0.2, 1.1, 1.5$	$x/h = 0.2, 1.5$
N-6	1.7 h	26 Sep. 1997	1300–1330	4.94	−26 deg	$x/h = -1.2, 0.7$	No measurement
N-7	1.7 h	26 Sep. 1997	1330–1400	4.94	−26 deg	$x/h = -1.2, 0.7$	No measurement

Table 2
Properties of the six white spruce trees examined during this study. Values in brackets are sample standard deviations

Tree no.	Tree height: z_t (m)	Stem diameter: dbh[a] (m)	Effective stiffness: K/C_0 ($m^2\ s^{-2}\ deg^{-1}$)	Damping coeff.: ζ	Natural freq.: ω_n (Hz)
1	12.1	0.19	*x*: 28.5 (2.8)	*x*: 0.083 (0.015)	*x*: 0.49 (0.03)
			y: 25.7 (3.2)	*y*: 0.089 (0.021)	*y*: 0.48 (0.01)
2	12.8	0.19	*x*: 106.6 (13.4)	*x*: 0.095 (0.019)	*x*: 0.49 (0.02)
			y: 63.6 (9.9)	*y*: 0.095 (0.018)	*y*: 0.45 (0.04)
3	13.1	0.22	*x*: 7.9 (1.3)	*x*: 0165 (0.032)	*x*: 0.30 (0.01)
			y: 14.0 (3.4)	*y*: 0.159 (0.020)	*y*: 0.33 (0.02)
4	14.6	0.30	*x*: 162.1 (26.0)	*x*: 0.108 (0.042)	*x*: 0.37 (0.01)
			y: 169.5 (43.9)	*y*: 0.140 (0.026)	*y*: 0.38 (0.01)
5	12.7	0.17	*x*: 24.5 (5.1)	*x*: 0.092 (0.012)	*x*: 0.43 (0.01)
			y: 13.5 (1.9)	*y*: 0.052 (0.004)	*y*: 0.44 (0.00)
6	17.2	0.19	*x*: 76.7 (6.1)	*x*: 0.153 (0.020)	*x*: 0.34 (0.01)
			y: —- —-	*y*: —- —-	*y*: —- —-
Ave.			63.0 (56.6)	0.112 (0.035)	0.41 (0.06)

Displacement properties are presented in both *x* and *y* directions. The *y* motion of tree 6 was not properly recorded.
[a]Diameter at Breast Height.

the across-cutblock direction (U_{clr}). In November 1995 we placed a 3-D propeller anemometer in the reference clearing to record turbulence characteristics.

2.3. Tree sway measurements

The sway of selected remnant white spruce trees was measured concurrently with 16 wind measurement periods (Table 1). Bi-axial tilt sensors (Mountain Watch, Calgary, AB), mounted on the stems at $z \approx 3$ m, gave angular displacements in the *x* and *y* directions (θ_x, θ_y). These were sampled at a frequency of 5 Hz, for durations of either 15 or 30 min. Two trees were measured during each observation period, with six trees measured in total: four near the centre of the wide cutblock, and one each at the upwind and downwind edge of the narrow cutblock (at $x/h = 0.2$ and 1.5). These trees were selected because they: (1) had a height near 15 m; (2) were isolated from other trees; and (3) were co-located (*x*-wise) with an anemometer. Selected trees were 30–60 m away from the anemometer transect lines. The height and diameter at breast height of the six measured trees are given in Table 2.

3. Modelling tree motion

We adopted a mechanical model of tree motion to relate winds to tree sway, but this was not absolutely necessary. A spectral approach can be used without employing a mechanical model, as discussed by Mayer (1987), by relying on a measured spectral transfer function to relate sway to the wind force spectrum.[1] This has the advantage of simplicity, and avoids characterising a tree mechanically. However, we believe that a mechanical model of tree sway provides a useful framework for analysis, allowing for more confident extrapolation of our results, and giving greater insight into tree behaviour. We modelled tree sway in the *x* and *y* direction separately using the *x*- and *y*-components of the wind force. In the following discussion, we demonstrate our analysis for the *x* direction only, although there was a completely analogous treatment of *y* motion.

3.1. Mass–spring–damper tree model

Trees respond to variable forcing with an oscillating motion. A mass–spring–damper model was taken as the simplest means of describing this behaviour. In our conceptual model (Fig. 2), the tree stem is a rigid rod which responds to the wind with an angular displace-

[1]Wind 'force' may be defined in different ways: as *u* at some point in the canopy (e.g. Gardiner, 1994); as the product of *u* and *w* above the canopy (e.g. Holbo et al., 1980); or as the height integral of the product of $u|u|$, foliage area, and a drag coefficient (Flesch and Grant, 1991).

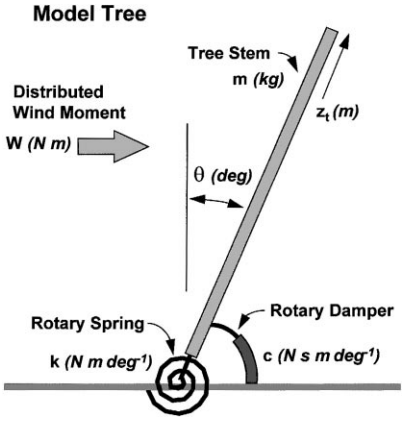

Fig. 2. Conceptual model of tree. Stem is a rigid rod with mass m, attached to the ground via a rotary spring having a spring constant k. Angular displacement (θ) is damped with a rotary damper having a damping constant c.

ment of the stem. Flexibility occurs via a rotary spring attachment to the soil, which is damped by a rotary dashpot. The tree has a mass m which is uniformly distributed over a height z_t.

Displacement in the x direction (θ_x), due to a distributed wind moment (W_x), is described by the following equation of motion:

$$\underbrace{\left(\frac{1}{3}\,m\,z_t^2\right)\frac{d^2\theta_x}{dt^2}}_{a1} + \underbrace{c\,\frac{d\theta_x}{dt}}_{a2} + \underbrace{k\,\theta_x}_{a3} - \underbrace{\left(\frac{m\,g\,z_t}{2}\right)\sin\theta_x}_{a4} = W_x(t) \quad , \tag{1}$$

where k is a spring constant ($N\,\mathrm{m\,deg^{-1}}$), c is a damping constant ($N\,\mathrm{s\,m\,deg^{-1}}$), and g is the gravitational acceleration. Terms al, a2, a3, and a4 are the moments of inertia, damping, spring, and displaced mass, respectively. The wind moment W_x ($N\,\mathrm{m}$) should properly be specified as the height integral of height multiplied by the wind force (see Eq. (6)). Assuming small displacements ($\sin\theta \cong \theta$), we defined $M = \mathrm{m}\ z_t^2/3$ and $K = k - \mathrm{m}gz_t/2$, so that Eq. (1) becomes:

$$M\frac{\mathrm{d}^2\theta_x}{\mathrm{d}t^2} + c\frac{\mathrm{d}\theta_x}{\mathrm{d}t} + K\theta_x = W_x(t) \tag{2}$$

If we specify $W_x = Kf_x$ (where f_x is a non-dimensional wind force), and divide Eq. (2) by M, we get the classic equation of motion for a mass–spring–damper system:

$$\frac{\mathrm{d}^2\theta_x}{\mathrm{d}t^2} + 2\zeta\omega_n\frac{\mathrm{d}\theta_x}{\mathrm{d}t} + \omega_\mathrm{n}^2\theta_x = \omega_\mathrm{n}^2 f_x(t), \tag{3}$$

where ζ is a non-dimensional damping coefficient ($\zeta = c/2\,M\,\omega_n$), and ω_n is the natural frequency of the tree ($\omega_\mathrm{n}^2 = K/M$). If the model tree is displaced and released, it oscillates at a frequency near ω_n, while ζ determines how quickly (in terms of a timescale c/M) the oscillations decay.

If the non-dimensional wind force is a simple cosine wave of frequency ω, where $f_x = (\beta/K)\cos\omega t$, the solution to Eq. (3) is (see Meirovitch, 1986)

$$\theta_x(t) = \frac{\beta}{K}|G(\omega)|\cos(\omega t - \Omega(\omega)), \tag{4}$$

with

$$|G(\omega)| = \frac{1}{\sqrt{\left(1-(\omega/\omega_\mathrm{n})^2\right)^2 + (2\zeta\omega/\omega_\mathrm{n})^2}},$$
$$\Omega(\omega) = \tan^{-1}\left(\frac{2\zeta\omega/\omega_\mathrm{n}}{1-(\omega/\omega_\mathrm{n})^2}\right). \tag{5}$$

The tree response is therefore a cosine wave with the same frequency as the wind force: the displacement amplitude is given by the transfer function $|G|$; and the displacement lags the input force by a phase lag Ω. Examples of $|G|$ and Ω are given in Fig. 3.

While the actual wind force W_x acting on a tree will not be a simple cosine wave, the solution expressed as

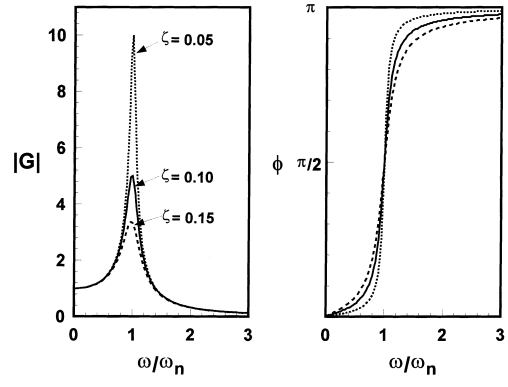

Fig. 3. Transfer functions $|G|$ and φ plotted vs. normalised frequency (ω/ω_n). These are for an ideal mass–spring–damper system.

Eq. (4) generalises to more complex cases. Since the mass–spring–damper model is linear, we can invoke superposition to determine the response to complicated forcing. If W_x is expressed as a Fourier series, then the total response of the tree is given by the sum of individual responses to each frequency component of W_x. At each frequency, Eqs. (4) and (5) describe that mode of displacement.

3.2. Estimating the wind moment

The wind moment W_x acting on a tree should be written as the height integral of the product of the drag coefficient (C_d), the tree frontal area density (A, $m^2\ m^{-1}$), and the relative wind velocity at the tree location ($u - z\,d\theta/dt$):

$$W_x(t) = \frac{1}{2}\rho \int_0^{z_t} C_D(z)A(z)\left(\left(u - z\frac{d\theta}{dt}\right)\left|\left(u - z\frac{d\theta}{dt}\right)\right|\right) z\,dz, \tag{6}$$

where ρ is air density. Application of this rigorous formulation requires height profiles of A, C_d, and U: comprehensive information that is rarely available, and was not available for this study. Instead, we assumed that W_x can be parameterised as proportional to $u|u|$ at a single reference location, here chosen as a point at our wind measurement height $z = 9$ m, and at the same x location as the tree in question ($u|u|_{x,z=9\,m}$). We also assumed that $u(z) \gg z\,d\theta/dt$, thus

$$W_x(x,t) = C_0(u|u|)_{x,z=9\,m}, \text{ or } f_x(x,t) = \frac{C_0}{K}(u|u|)_{x,z=9\,m} \tag{7}$$

where C_0 (kg) is an aggregate drag constant,

$$C_0 = \frac{1}{2}\rho\left(\int_0^{z_t} C_d(z)A(z)u(x,z)|u(x,z)|z\,dz\right)\Big/(u|u|)_{x,z=9\,m}. \tag{8}$$

The value of C_0 will vary from tree to tree due to differences in z_t and A. It would also change if one were to choose an alternative reference height for the wind velocity input.[2] The ratio C_0/K, which we later define as the reciprocal of tree 'stiffness,' is in essence a proportionality constant which relates $u|u|$ to tree displacement. Hereafter, $u|u|$ will refer to velocity measurements taken at $z = 9$ m and at a specific x location, and we drop the subscript (x, $z = 9$ m).

Our analysis of tree motion relied on expressing the wind force as a Fourier series. A discrete time series of $u|u|$, providing N observations over time T (with a sampling interval Δt), was written as a finite Fourier series (Chatfield, 1984):

$$u|u|(t) = \langle u|u|\rangle + \left(\sum_{p=1}^{(N/2)-1} R_{u|u|}(p\omega_0)\cos(2\pi p\omega_0 t + \varphi_{u|u|}(p\omega_0)\right) + a_{N/2}\cos(\pi t/\Delta t), \tag{9}$$

where $\omega_0 = 1/T$, $R_{u|u|}(p\omega_0)$ and $\varphi_{u|u|}(p\omega_0)$ are the amplitude and phase of the pth harmonic, and $\langle u|u|\rangle$ is the time average of $u|u|$. The coefficient $a_N/2$, defined as $\Sigma(-1)^{t/\Delta t}u|u|(t)/N$, is usually small and was thus neglected. We defined the power spectrum $S_{u|u|}$ as

$$S_{u|u|}(p\omega_0) = R^2_{u|u|}(p\omega_0)/(2\omega_0), \tag{10}$$

so that

$$\sigma^2_{u|u|} = \sum_{p=1}^{(N/2)-1} S_{u|u|}(p\omega_0)\omega_0 \tag{11}$$

Power spectra were obtained by standard Fourier analysis, and smoothed using a simple moving average. At each location we created an ensemble-averaged spectrum from the five or six observed $u|u|$ spectra, making the transform to wavenumber $\kappa = \omega/S_{clr}$. The basis for using this transform is the belief that turbulent eddies in the forest environment have invariant spatial dimensions (which scale on h). While increasing wind speeds advect these eddies more rapidly, therefore shifting $S_{u|u|}$ toward higher frequencies, a power spectral density defined in terms of wavenumber, $S_{u|u|}(\kappa)$, remains invariant.[3]

[2] C_0 will also vary with time for a single tree: C_d and A are likely to be velocity-dependent (Thom, 1971), and the shape of the instantaneous velocity profile may also exhibit variability.

[3] In fact it was not clear whether $S_{u|u|}$ showed smaller sampling variation when plotted versus κ or ω. The range of S_{clr} in our experiment was relatively small, so the superiority of scaling with respect to κ may not have been apparent.

3.3. Estimating ζ, ω_n and K/C_0

A determination of ζ, ω_n, and an equivalent stiffness (K/C_0) is necessary to apply the mass–spring–damper model. This was done by reconciling the model transfer function $|G|$ with the measured power spectra of tree displacement ($S_{\theta x}$) and wind force ($S_{u|u|}$). In our mass–spring–damper model, $S_{\theta x}$ and $S_{u|u|}$ are related by the simple algebraic expression,

$$S_{\theta x}(\omega) = \left(\frac{C_0}{K}\right)^2 |G(\omega)|^2 S_{u|u|}(\omega), \qquad (12)$$

where $|G(\omega)|$ is given by Eq. (5). We can calculate a 'measured' transfer function by rearranging Eq. (12),

$$|G(\omega)|_{\text{meas.}} = \frac{K}{C_0}\sqrt{S_{\theta x}(\omega)/S_{u|u|}(\omega)}. \qquad (13)$$

If the mass–spring–damper model was accurate, and $u|u|$ was the exact wind force acting on the tree, then $|G(\omega)|_{\text{meas.}}$ should exactly equal $|G(\omega)|$, so that

$$\frac{(C_0/K)^2}{\left(1-(\omega/\omega_n)^2\right)^2+(2\zeta\omega/\omega_n)^2} = S_{\theta x}(\omega)/S_{u|u|}(\omega) \qquad (14)$$

One could then solve for K/C_0, ζ and ω_n. Since our observations of tree sway were made at a different y location than were our observations of the wind, and because $S_{\theta x}$ and $S_{u|u|}$ were 'noisy,' the function $S_{\theta x}$ and $S_{u|u|}$ was not smooth. Values of K/C_0 ζ and ω_n were found by iteration, minimizing the error between the (modelled) left hand side of Eq. (14), and the (measured) right hand side. This fitting exercise was confined to $\omega < 0.6$ Hz, due to the inaccuracy of the mass spring–damper model at higher frequencies (as discussed below).

3.4. Predicting tree sway

With values of ζ, ω_n and K/C established, the mass–spring–damper model allows prediction of θ_x from a time series of $u|u|$. Our approach was to predict the variance of sway angle, and the maximum sway angle, for our characteristic tree during a 'characteristic' 15 min time period (defined by the ensemble average $S_{u|u|}/\sigma^2_{u|u|}$). The variance of θ_x (with N observations over time T), is given by:

$$\frac{\sigma^2_{\theta_x}}{C_0/K^2} = \sum_{p=1}^{(N/2)-1} |G(p\omega_0)|^2 S_{u|u|}(p\omega_0)\omega_0, \qquad (15)$$

where $\omega_0 = 1/T$. A discrete θ_x time series is implied by the $S_{u|u|}$ and $\varphi_{u|u|}$ spectra:

$$\frac{\theta_x(t)}{C_0/K} = \langle u|u|\rangle + \sum_{p=1}^{(N/2)-1} |G(p\omega_0)|\sqrt{2\omega_0 S_{u|u|}(p\omega_0)} \times \cos\left(2\pi p\omega_0 t + \varphi_{u|u|}(p\omega_0) - \Omega(p\omega_0)\right). \qquad (16)$$

Eq. (16) allows us to predict a maximum displacement ($\theta_{x\max}$) from a $u|u|$ time series. Eqs. (15) and (16), and their equivalents in the y direction, were employed at three locations in the narrow cutblock, five locations across the wide cutblock, and in the reference clearing. The steps used to make sway predictions were as follows.

1. Select an average wind velocity U_{clr} in the reference clearing ($S_{\text{clr}} \simeq U_{\text{clr}}$). We considered the case of winds oriented directly across the cutblock ($V = 0$, $\langle v|v|\rangle = 0$).
2. Assign $\langle u|u|\rangle$, $\sigma_{u|u|}$, and $\sigma_{v|v|}$ values at each location based on our observations of the value of $\langle u|u|\rangle/U_{\text{clr}}{}^2$, $\sigma_{u|u|}/U_{\text{clr}}{}^2$, and $\sigma_{v|v|}/U_{\text{clr}}{}^2$.
3. Convert the ensemble-average wavenumber-based $S_{u|u|}(K)/\sigma^2_{u|u|}$ and $S_{v|v|}(K)/\sigma^2_{v|v|}$ at each location to the frequency based $S_{u|u|}(\omega)$ and $S_{v|v|}(\omega)$.
4. Calculate $\sigma_{\theta x}$ using Eq. (15), then create $\sigma_{\theta y}$. The total displacement variance is defined as:
$$\sigma^2_\theta = \sigma^2_{\theta_x} + \sigma^2_{\theta_y}. \qquad (17)$$
5. Calculate 15 min time series of θ_x using Eq. (16), from which $\theta_{x\max}$ is determined (five or six time series of θ_x were created for each location, using the ensemble-average $S_{u|u|}$ combined with the five or six observed $\varphi_{u|u|}$ spectra, from which an average $\theta_{x\max}$ was calculated). A simultaneous θ_y time series was created from the $v|v|$ spectra. The maximum displacement is calculated as:
$$\theta_{\max} = \text{maximum}\sqrt{\theta^2_x(t) + \theta^2_y(t)}. \qquad (18)$$

3.5. Accuracy of the tree model

How well does a simple mass–spring–damper model describe tree sway? Reasonably well, based

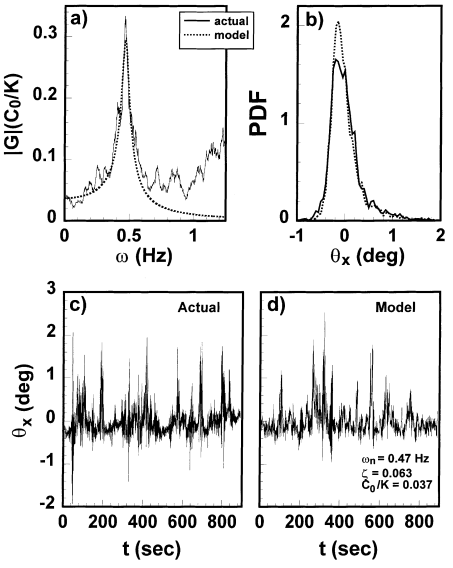

Fig. 4. Comparison of actual and modelled tree displacement (x direction) during a 15 min observation period: (a) the normalised transfer function $|G|(K/C_0)$ plotted vs. frequency ω; (b) the probability density function (PDF) of the fluctuating displacement $(\theta_x - \langle\theta_x\rangle)$; (c) the actual displacement time series; and (d) the displacement time series from the mass–spring–damper model in response to the measured $u|u|$ forcing.

on the agreement between the model transfer function $|G|$ (Eq. (5)) and the measured transfer function $|G|_{\text{meas}}$ (Eq. (13)). Fig. 4(a) illustrates this agreement for one tree during one of our 15 min measurement periods. The result was typical, with $|G|_{\text{meas}}$ closely resembling $|G|$ for $\omega \leq 0.6$ Hz. The sharp peak in $|G|_{\text{meas}}$ near $\omega = 0.5$ Hz corresponds to the natural frequency of the tree (ω_n). A more stringent test of model fidelity is the comparison of modelled sway angle $\theta_x(t)$ (from, Eq. (16)) with an actual displacement time series. Fig. 4(c,d) shows such a comparison. The two series should not be identical. The wind observations were made more than 30 m from the actual tree, so that $u|u|$ should correspond to the actual forcing on the tree only in a statistical sense (rather than a deterministic sense). We considered that there was tolerable agreement between the actual and reconstructed sway, as reflected in agreement between the actual and modelled probability density function (PDF) for θ_x (Fig. 4(b)).

While the tree illustrated in Fig. 4 exhibited mass–spring–damper behaviour at low frequencies, this was not the case for $\omega > 0.6$ Hz. The poor fidelity of our model at high frequencies was partially the result of the tree being a continuous system (as opposed to our single degree-of-freedom model), possessing many vibrating modes and a corresponding number of natural frequencies above the fundamental natural frequency. Vibrations at these higher natural frequencies would appear as secondary peaks in $|G|$. Our observations showed a consistent secondary peak in $|G|$ at two or three times the fundamental peak. Another contribution to the poor high frequency performance of our too simple model may be the shaking branches of the trees, which transmit high frequency motion to the stem.

Given our focus on windthrow, we believe that a mass–spring–damper model is a good choice to describe tree sway, despite its inaccuracy at high frequencies. The model gives an accurate description of stem motion (at a single point) for frequencies up to, and including the fundamental natural frequency. All indications are that tree sway in the fundamental mode is the predominant form of motion, and is responsible for windthrow. For instance, Wood (1995) analysed a composite Sitka spruce tree and found that vibration in the fundamental mode resulted in maximum stress at the ground (consistent with uprooting), while the second mode vibration resulted in a maximum stress at 80% of the tree height, and is therefore unlikely to explain uprooting.

4. Wind forces in the cutblocks[4]

4.1. Average of wind force

The average alongwind wind 'force' ($\langle u|u|\rangle$) in the cutblocks was significantly reduced relative to concomitant values in the nearby large reference clearing (Fig. 5). In the cutblocks, $\langle u|u|\rangle$ was never greater than 25% of the corresponding value in the reference clearing (for winds oriented across the cutblock). The average displacement of our characteristic remnant spruce in the cutblocks would therefore be less

[4]Our measurements of $u|u|$ were subject to errors due to the poor high frequency response of the propeller anemometers. These errors, and our correction to the $u|u|$ time series, are discussed in the Appendix A.

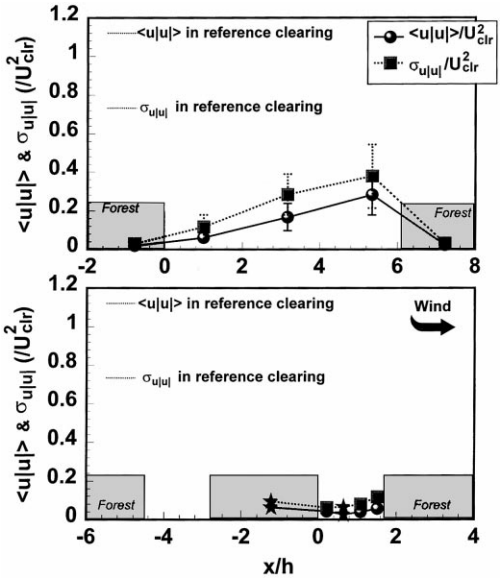

Fig. 5. The average across-cutblock wind force <$u|u|$> and standard deviation $\sigma_{u|u|}$, scaled on the average velocity in the reference clearing (U_{clr}), plotted vs. x across the wide cutblock (top) and the narrow cutblock (bottom). The average wind direction was across the cutblock (along x direction, ± 30 deg). The 'error bars' surrounding each observation are ± one standard deviation. Values of normalised <$u|u|$> and $\sigma_{u|u|}$ in the reference clearing are shown by the level dashed line.

than 25% of that in the clearing (since $\langle\theta_x\rangle \propto \langle u|u|\rangle$). In terms of average tree displacement, the cutblocks provided very effective shelter.

The pattern of $\langle u|u|\rangle$ across the cutblocks was as expected, given the velocity statistics described in the first paper of this series (Flesch and Wilson, 1999), noting that $\langle u|u|\rangle \approx \langle u^2\rangle \equiv U^2 + \sigma_u^2$. Upwind of the wide cutblock (x/h = −0.8), ⟨u|u|⟩ was only 2% of that in the reference clearing. Its value increased steadily with x across the cutblock, reaching 25% of the clearing value at x/h = 5.4, before rapidly decreasing into the downwind forest. In the narrow cutblock, $\langle u|u|\rangle$ remained at only 3–5% of the clearing values. Interestingly, we observed an initial decrease in $\langle u|u|\rangle$ with in the narrow cutblock, so that the minimum $\langle u|u|\rangle$ lay at x/h = 1.1.

4.2. Turbulent wind force

Fig. 5 also shows the (normalised) standard deviation $\sigma_{u|u|}$ of the wind force across the cutblocks. An increase in $\sigma_{u|u|}$ would indicate an increase in the peak wind force, and correlate with increased tree sway. Compared with the reference clearing, $\sigma_{u|u|}$ in the cutblocks was reduced, but not by so large a factor as was $\langle u|u|\rangle$. In the forest upwind of our cutblock (x/h = −0.8), $\sigma_{u|u|}$ was only 4% of the clearing value. Its value increased to 50% at x/h = −5.4 in the wider cutblock, before falling rapidly in the downwind forest. In the narrow cutblock $\sigma_{u|u|}$ remained at low levels, ranging from 8 to 16% of the clearing values. The pattern of $\sigma_{u|u|}$ differed from that of σ_u, which was described in Flesch and Wilson (1999). While σ_u in the cutblock reached or exceeded its value in the reference clearing, $\sigma_{u|u|}$ remained well below its clearing value (because the average velocity U, a component of $\sigma_{u|u|}$, remained well below its clearing value). The across-wind force fluctuations ($\sigma_{v|v|}$) exhibited a pattern similar to $\sigma_{u|u|}$. In the wide cutblock $\sigma_{v|v|}$ was approximately 60% of $\sigma_{u|u|}$. In the narrow cutblock, the magnitudes of $\sigma_{u|u|}$ and $\sigma_{v|v|}$ were nearly equal.

4.3. Power spectra

Our observations showed that the sheltered cutblocks provided an environment where wind forces were reduced compared with large clearings. However, the frequency characteristics of the turbulent wind force are also important in determining the effectiveness of wind shelter at reducing tree sway. Fig. 6 shows ensemble-averaged power spectra of the wind force ($S_{u|u|}/\sigma^2{}_{u|u|}$) at different cutblock locations. These normalised spectra do not reflect differences in the magnitude of $u|u|$ fluctuation between locations, only differences in the relative wavenumber contributions (e.g. because $\sigma^2_{u|u|}$ in the clearing was 600 times greater that in the forest, $S_{u|u|}$ in the clearing greatly exceeded that in the forest at all wavenumbers). The $S_{u|u|}/\sigma^2{}_{u|u|}$ had a shape as expected, with the greatest 'power' at the lowest wavenumbers.

The higher frequency range is of most interest when considering tree sway. Trees will respond preferentially to $u|u|$ in the frequency range near ω_n, and literature values of ω_n generally exceed 0.1 Hz. The inset of Fig. 6 focuses on $S_{u|u|}/\sigma^2{}_{u|u|}$ from $\kappa = 0.02$ to 0.05 m^{-1} (this corresponds to $\omega = 0.2$–0.5 Hz when $S_{clr} = 10\ m\ s^{-1}$). Two trends were evident in this wavenumber region. First, the high wavenumber contributions to $u|u|$ were larger in the narrow cutblock

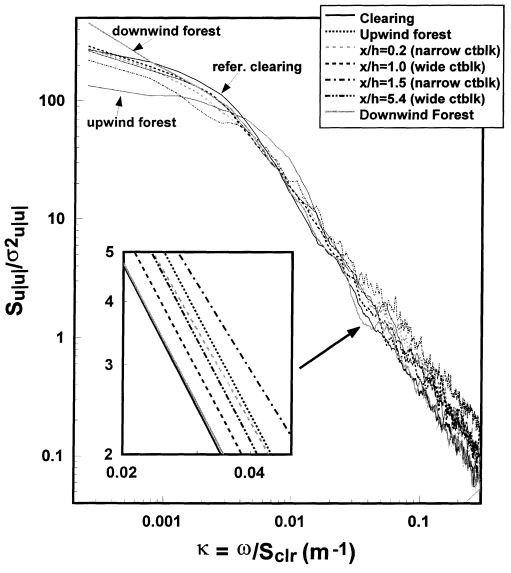

Fig. 6. Ensemble-averaged power spectra of the across-cutblock wind force ($S_{u|u|}$), scaled on the variance of $u|u|$ ($\sigma^2_{u|u|}$), and plotted vs. wavenumber $\kappa(=\omega/S_{clr})$. Different lines represent spectra at different locations in the wide and narrow cutblocks. Inset is the geometric fit to the spectra in the κ range corresponding to the tree natural frequency.

than in the wide cutblock, which were in turn larger than in the clearing. Second, within each cutblock there was an increase in the high wavenumber contribution with increasing downwind distance x. We can therefore speculate that the 'effectiveness' of the wind in generating tree sway varies with cutblock location. The wind effectiveness would be lowest in the clearing, and highest in the narrow cutblock. So while the sheltered cutblock provided an environment of reduced $\langle u|u|\rangle$ and $\sigma_{u|u|}$, this was accompanied by an increase in the effectiveness of the wind at creating tree sway (we show later, however, that the differences in wind 'effectiveness' did not significantly change the fact that sway at all locations was well correlated with $\sigma_{u|u|}$).

5. Modelled tree sway

5.1. 'Characteristic' remnant spruce

The effective stiffness (K/C_0), natural frequency (ω_n) and damping coefficient (ζ) of the six remnant spruce examined in our study are shown in Table 2. The average K/C_0 was 63 m^2 s^{-2} deg^{-1}, with a standard deviation of almost the same magnitude. This high variability was expected, given the high variability in tree features which affect K and C_0: differences in tree height, stem diameter, soil strength, and root patterns all affect the stiffness K; and differences in tree height and foliage amount and distribution affect the effective drag coefficient (C_0). There was considerably less variation in ζ and ω_n. Among the six trees, ζ averaged 0.11, with a standard deviation of 0.04. The average ω_n was 0.41 Hz, with a standard deviation of 0.06 Hz.

While we observed directional differences in these characteristics for each tree, they were not consistent (e.g. some trees were stiffer in the x direction, others in the y direction). When we compare these values of ζ and ω_n with values found in other studies of similar trees (Table 3), we conclude that our 'characteristic' remnant spruce had a ω_n within the expected range, although it was more heavily damped than expected.

5.2. Sway characteristics

Using the mass–spring–damper model, we predicted remnant tree sway over a 'characteristic' 15 min period (defined by the ensemble average $S_{u|u|}/\sigma^2_{u|u|}$ and $S_{v|v|}/\sigma^2_{v|v|}$) for the case of winds oriented

Table 3
The natural frequency (ω_n) and damping coefficient (ζ) of trees reported in the literature

Tree-type	z_t (m)	dbh (m)	ω_n (Hz)	ζ	Reference
White spruce	12–17	0.17–0.30	0.30–0.49	0.05–0.17	This study
Sitka spruce	13–14	0.14–0.21		0.01–0.05	Blackburn et al. (1988)
Sitka spruce	13–15	0.11–0.18	0.26–0.40	0.06–0.07	Milne (1991)
Sitka spruce	10–14	0.10–0.18	0.39–0.47	0.04–0.08	Gardiner (1995)

These trees had a similar height (z_t) and stem diameter (dbh: diameter at breast height) as our study trees.

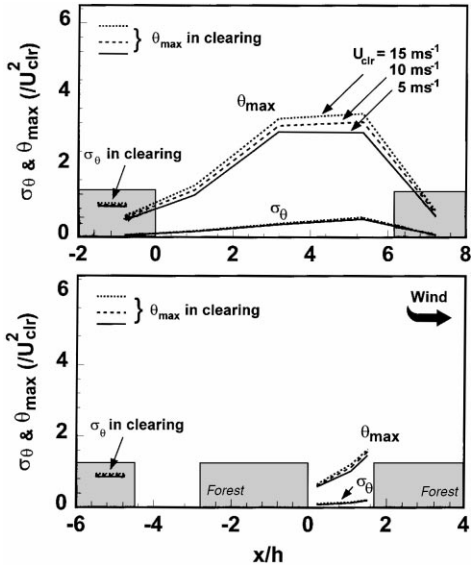

Fig. 7. Predictions of the standard deviation of tree sway (σ_θ) and maximum displacement (θ_{max}) of our characteristic tree at three different reference clearing velocities (U_{clr}), plotted vs. x across the wide cutblock (top) and narrow cutblock (bottom). Displacements are scaled on U^2_{clr} (the stiffness K/C_0 has been absorbed in θ). Also shown (in level lines) are σ_θ/U^2_{clr} and θ_{max}/U^2_{clr} for that tree when located in the reference clearing.

across the cutblock. Our characteristics tree was defined to have $\zeta = 0.11$ and $\omega_n = 0.4$ in both the x and y directions. Since our interest was in the spatial variation of the sway of a single reference tree, not absolute displacements, we did not define a characteristic stiffness K/C_0. Hereafter, we report displacements scaled on C_0/K (the units of the scaled θ are $m^2\ s^{-2}$). We emphasise that the following results are predictions (not measurements) of tree sway, founded on the measured wind plus the (now calibrated) tree model. Actual tree displacements were used only in the development of the tree model. Although we have shown model skill at replicating actual tree displacements, an uncertainty follows from the use of a model.

Fig. 7 shows our predictions of tree sway, in the form of the normalised standard deviation of displacement $\sigma_\theta/U_{clr}{}^2$, and normalised maximum displacement $\theta_{max}/U_{clr}{}^2$ (recall that the factor C_0/K has been absorbed in θ). Two features are evident: the effect of increasing ambient wind velocity on sway, and the change in sway magnitude with location. Our predictions show that increasing ambient wind velocity increases the sway more than the corresponding increase in wind forces. On average $\sigma_\theta/U_{clr}{}^2$ was about 10% higher when U_{clr} was 15 m s^{-1} compared with 5 m s^{-1}, and $\theta_{max}/U_{clr}{}^2$ was about 15% higher (these ratios would remain unchanged if sway were purely proportional to wind force). This sway 'amplification' is attributed to an increase in wind 'power' at frequencies near ω_n – an increase in U_{clr} shifts $S_{u|u|}$ toward higher frequencies. This was a consequence of our assumption that $S_{u|u|}/\sigma_{u|u|}{}^2$ and $S_{v|v|}/\sigma_{v|v|}{}^2$ were invariant when plotted with wavenumber κ, and therefore this result should not be taken as an independent observation. As the sensitivity of tree sway to U_{clr} was predicted to be roughly the same at all locations, the relative sway in the cutblocks (i.e. sway relative to an identical tree in the clearing) was insensitive to U_{clr}. We therefore predict that the shelter effectiveness (given by relative sway) will not change with changing ambient windspeed.

The most distinctive feature in Fig. 7 is the increase in both σ_θ and θ_{max} with increasing x across the cutblocks. In the forest immediately upwind of our wide cutblock, we calculated that σ_θ would be 6% of the corresponding value for that tree if located in the clearing (with no inter-tree contact), implying excellent wind shelter. By $x/h = 5.4$, σ_θ had reached approximately 60% of its value in the reference clearing. The value of σ_θ then fell rapidly in the downwind forest. The pattern of maximum displacement was slightly different. The θ_{max} varied from 10% of its clearing value in the upwind forest, to 57% at $x/h = 3.2$; however, there appeared to be a plateau between $x/h = 3.2$ and 5.4. As expected, both σ_θ and θ_{max} in the narrow cutblock were low, ranging from 10 to 30% of their clearing values. Other features of predicted sway in the cutblocks included:

1. The average displacement $\langle\theta_x\rangle$ was small compared with the maximum displacement, with $\theta_{xmax}/\langle\theta_x\rangle \approx 20$. This was larger than the value of 10 measured by Stacey et al. (1994) in a wind tunnel model forest. At our reference clearing $\theta_{xmax}/\langle\theta_x\rangle \approx 5$.
2. Relative to the clearing, θ_{max} was never reduced by as much as was σ_θ. This reflects the intermittent nature of the cutblock winds, where the maximum gust velocities are not reduced to the same fractional extent as the reduction in U of σ_u.

3. The ratio $\theta_{max}/\sigma_\theta$ ranged from 5 to 10. It was highest in the forest, lowest in the reference clearing, and ranged from 6 to 8.5 in the cutblocks. This ratio was predicted to increase slightly with increasing $U_{clr.}$

We can infer from the tree model that a significant amount of tree motion can be labelled as 'resonant sway.' In a 'static' system the displacement is proportional to the driving force, so that $\sigma_{\theta x}/\sigma_{u|u|} = \theta_{x\max}/u|u|_{\max} = 1$ (recall the stiffness K/C_0 has been absorbed in θ). But as $u|u|$ fluctuates, these ratios can exceed one due to $u|u|$ forcing near ω_n. We define this additional motion as 'resonant sway.' Our characteristic tree exhibited resonant sway in the cutblocks, as $\sigma_{\theta x}/\sigma_{u|u|} = \theta_{x\max}/u|u|_{\max}$ ranged from 1.10 to 1.35. In other words, the interaction of the turbulence with tree dynamics increased displacements 10–35% over that expected from a static analysis of the wind.

Our predictions of resonant sway support the conclusion of Stacey et al. (1994), that the dynamic nature of tree response results in greater maximum displacement than if the response were static. However, the increased sway that we diagnosed was less than that calculated by Stacey et al. for model trees. They calculated a doubling of the standard deviation of tree displacement due to resonant sway, compared with our increase of 10–35%. This was not unexpected given that there were differences between our tree heights (z_t = h vs. z_t = 0.5 h), and tree locations (full canopy vs. cutblock). Our predictions of the magnitude of resonant sway were also at odds with the suggestion made by Blackburn et al. (1988). They suggested a 'dynamic load factor' (roughly equivalent to $\sigma_{\theta x}/\sigma_{u|u|}$ and $\theta_{x\max}/u|u|_{\max}$) of half the 'resonant load factor' (the maximum value of $|G|$) be used to estimate tree response to the wind. In our case (where the maximum $|G|$ was approximately 5), this would have resulted in an overprediction of tree sway by roughly a factor of two.

5.3. Sensitivity to ζ and ω_n

Given the 'dynamic' response of trees to the turbulent wind force, one expects ζ and ω_n to strongly influence the sway characteristic. This was certainly true in terms of 'absolute' sway predictions (Fig. 8).

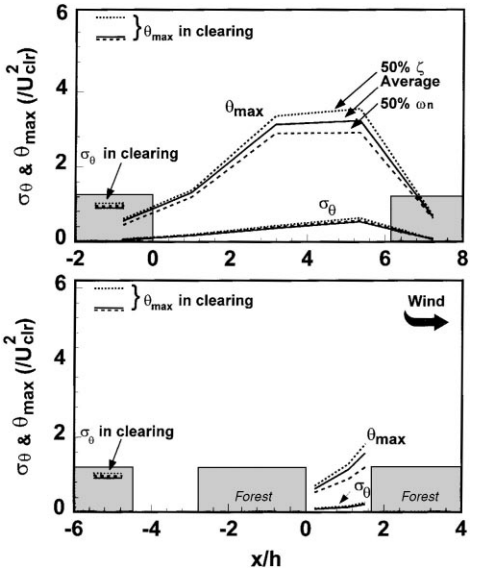

Fig. 8. Predictions of the standard deviation of tree sway (σ_θ) and the maximum displacement (θ_{max}), plotted vs. x across the wide cutblock (top) and the narrow cutblock (bottom). Different lines are for: a tree having the average damping coefficient (ζ) and natural frequency (ω_n) we observed (denoted 'Average'); a tree having ζ reduced to 50% of the observed average (denoted '50% ζ'); and a tree having ω_n reduced to 50% of the observed average (denoted '50% ω_n'). Displacement are scaled on U^2_{clr}, where θ has been scaled on C_0/K. Also shown (in level lines) are σ_θ/U^2_{clr} and θ_{max}/U^2_{clr} for these trees when located in the reference clearing.

When ζ was reduced 50%, σ_θ in the cutblocks increased by 17–23%, and θ_{max} increased by 5–16%. When ω_n was reduced 50%, σ_θ increased by 3–9%, although θ_{max} decreased by 8–24%.[5] Nonetheless, the relative sway (sway relative to that of an identical tree sited in the clearing) was insensitive to ζ and ω_n. This is illustrated in Fig. 9, which shows the ratios of σ_θ and θ_{max} to their values in the reference clearing. The insensitivity of these ratios to ζ and ω_n can be traced to the similarity in the shape of $S_{u|u|}$ and $S_{v|v|}$ at the different locations (e.g. if ω_n is decreased, the increase in wind 'power' at frequencies near ω_n is proportionally the same at all locations). While earlier we documented differences in $S_{u|u|}$ with location, these differences were clearly not significant in terms of sway response. From these predictions we conclude

[5] This was contrary to expectations that greater θ_{max} accompanies greater σ_θ. Apparently a lower ω_n results in a more 'sluggish' tree, less responsive to maximum $u|u|$ events.

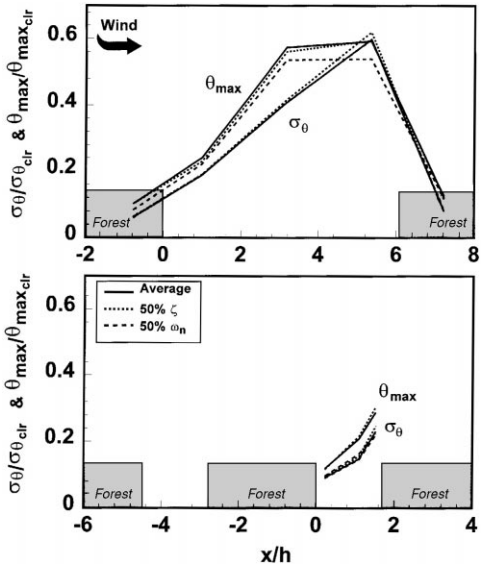

Fig. 9. Ratio of tree sway in cutblocks to the corresponding sway in the reference clearing (for σ_θ and θ_{max}). Different lines are for: a tree having the average damping coefficient (ζ) and natural frequency (ω_n) we observed (denoted 'Average'); a tree having ζ reduced to 50% of the observed average (denoted '50% ζ'); and a tree having ω_n reduced to 50% of the observed average (denoted '50% ω_n').

that the effectiveness of a cutblock shelter in reducing tree sway will not depend on the dynamical properties of the remnant spruce.

5.4. Relationship of tree sway to simple wind statistics

Our diagnoses of tree sway required a spectral analysis of u and v time series, and a model of tree motion. Is there a simpler means of determining tree sway? The insensitivity of relative sway (sway relative to an identical tree in the reference clearing) to tree dynamics suggests that wind statistics alone may provide a way to discriminating regions of high and low tree sway. We believe $\sigma_{u|u|}$ to be a good index of relative sway, as we found it to be highly correlated with predictions of both σ_θ and θ_{max}. For example, the ratio $\sigma_\theta/\sigma_{u|u|}$ was relatively constant in the cutblocks (1.56 ± 0.22). The ratio $\theta_{max}/\sigma_{u|u|}$ was only slightly more variable (11.4 ± 2.8). If we were to change ζ and ω_n, these ratios would change, but their values would remain relatively constant with location.

As statistics of $u|u|$ have not been reported in the literature, it is useful to relate $\sigma_{u|u|}$ to ordinary wind velocity statistics of which we are more knowledgeable. We found that $\sigma_{u|u|}$ can be approximated by ${\sigma_u}^2$ (to within 4% at all locations), so that

$$\frac{\sigma^2_{u|u|}}{\sigma^4_u} \approx \frac{\sigma^2_{u^2}}{\sigma^4_u} = Kt_u - 1 + 4\left(\frac{U}{\sigma_u}\right)^2 + 4\left(\frac{U}{\sigma_u}\right)Sk_u\,, \quad (19)$$

where Kt_u and Sk_u are the skewness and kurtosis of u. If U, σ_s, Sk_u, and Kt_u can be accurately estimated, either by an educated guess, measurements, or by a wind flow model, then $\sigma_{u|u|}$ can be estimated (and thus by implication σ_θ and θ_{max}).

With the expectation that Sk and Kt would be more difficult to predict than U and σ_u, we calculated $\sigma_{u|u|}$ from just our observations of U and σ_u, assuming Gaussian values of $Sk_u = 0$ and $Kt_u = 3$. The result was a 18–29% underestimation of $\sigma_{u|u|}$ in the cutblocks. Using more realistic values of $Sk_u = 1$ and $Kt_u = 4$ (i.e. values around the average of those we observed), the estimates of $\sigma_{u|u|}$ improved to within 6% of the actual $\sigma_{u|u|}$. This leads us to conclude that accurate estimates of variation in Sk_u and Kt_u are not very important in estimating $\sigma_{u|u|}$. We believe that constant, non-Gaussian, values of Sk_u and Kt_u can be used with good accuracy to determine $\sigma_{u|u|}$ via Eq. (19)

6. Estimating shelter effectiveness

If windthrow is the result of tree sway exceeding a critical value, then our sway predictions can be used to quantify the effectiveness of sheltered cutblocks at reducing windthrow of remnant spruce. Our approach was to predict a threshold average wind velocity (U_w,) measured in our large reference clearing; essentially a weather station windspeed) which correlates with the occurrence of windthrow in the cutblocks. Our *assumption* was that an average velocity of 10 m s^{-1} causes windthrow of unprotected trees in our large reference clearing (Dr. S. Navratil, 1994, Canadian Forest Service, pers. commun.). Larger windspeeds (U_w) ought to be needed to cause windthrow in the cutblocks.

The pattern of U_w in the cutblocks is illustrated in Fig. 10. In the wide cutblock U_w ranged from 25 m s^{-1} in the upwind portion of the cutblock, to

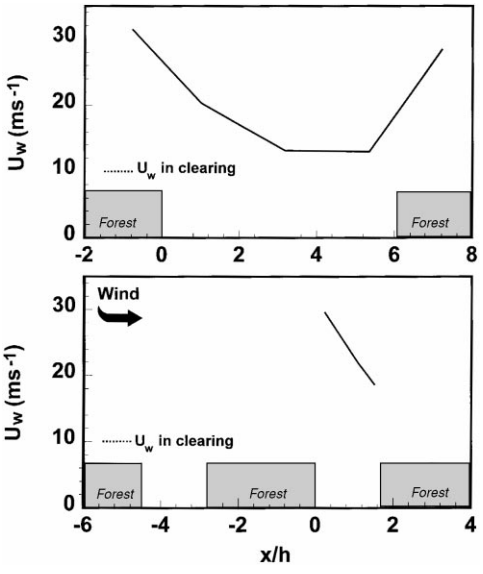

Fig. 10. Predictions of the threshold average wind velocity measured in the open (U_w, essentially a weather station windspeed), which correlates with the occurrence of windthrow of remnant spruce in the cutblocks. Our *assumption* was that a U_w of 10 m s^{-1} causes windthrow of unprotected trees in the open. Larger wind velocities (U_w) are needed to cause windthrow in the cutblocks.

13 m s^{-1} at the downwind edge. This means that windthrow at the upwind edge of the cutblock would require a weather station windspeed of 25 m s^{-1}, compared with the much lower 10 m s^{-1} needed in our large clearing. Even the least protected zone of the wide cutblock would require a 30% higher wind velocity to cause windthrow than is needed in the large clearing. The difference in U_w between $x/h = 3.2$ and 5.4 was slight, indicating that the most effective windthrow protection occurs in the region $x/h < 3$. The wind shelter in the narrow cutblock was impressive, with U_w ranging from 30 m s^{-1} (upwind) to 19 m s^{-1} (downwind).

How significant is the level of wind shelter in the cutblocks? From an extreme value analysis of wind gusts, we estimate that an average windspeed of 11 m s^{-1} is expected every 2 years at the Hotchkiss site,[6] a 13 m s^{-1} windspeed would occur every 5 years, while a windspeed of 15 m s^{-1} is expected only every 20 years. This suggests that windthrow in the narrow cutblock, or in the upwind portion of the wide cutblock (where the critical U_w>15 m s^{-1}), would rarely occur.

Our map of windthrow velocity thresholds across the cutblocks was based on the assumption that our characteristic tree is mechanically identical at all locations. However, we expect ζ to be higher in the clearing because of increased aerodynamic damping due to the higher winds it would experience, and C_0 might differ because of differences in the shape of the vertical wind profile at each location. Furthermore, trees adapt to higher wind exposure, and the remnant spruce in a large clearing would eventually differ from those in a cutblock. Therefore our assignment of a U_w would at best be valid only for a short time after harvest – however, it is this post-harvest period that is critical for windthrow.

Given the uncertainty in our assumptions, and bearing in mind the wide range of remnant tree-types (with properties varying substantially from our 'characteristic' tree), the actual magnitude of our U_w values must be viewed skeptically. However, we feel confident that the pattern exhibited in Fig. 10 exists, with most effective shelter occurring within three tree heights of the upwind forest.

7. Conclusions

Our diagnoses of tree sway confirm what we speculated in the first paper of this series: that the most effective windthrow shelter for remnant understory spruce is within three tree heights of the upwind forest – corresponding to the 'quiet zone.' This result holds irrespective of the dynamic parameters (ω_n and ζ) of our characteristic tree, or strength of the ambient wind velocity. We believe it has generality to other cutblock dimensions and forest-types, since the wind regime in our cutblocks was generally consistent with observations taken in a wide range of cutblocks/clearings (see Flesch and Wilson, 1999). In designing shelterwood harvest systems to reduce windthrow of remnant understory spruce, we therefore suggest cutblocks should not exceed three tree heights in width (at least when cutblocks have an upwind forest border greater than 2 h). While wind shelter should exist beyond this distance, remnant trees so far from the upwind shelter

[6]This was based on maximum wind gust statistics at nearby High Level, Alberta (Flesch and Wilson, 1993).

would not be dramatically more protected than if they were exposed in a large clearing.

Our results cannot be used to predict the shelter effectiveness of *any* possible shelterwood harvest design. For example, our results tell us little about the sensitivity of windthrow protection to the width of the upwind forest border; and we cannot be sure that a dramatically different forest structure, or different topography, would uphold the features we observed. We believe that a wind flow model is the best avenue for investigating the range of possible harvest designs. We have shown that the wind statistics generated by a typical flow model (e.g. U and σ_u) can be used to estimate $\sigma_{u|u|}$, which is a good predictor of tree sway and therefore, we believe, windthrow potential. The formulation of a wind flow model appropriate to forest cutblocks is reported in the final paper of this series (Wilson and Flesch, 1999).

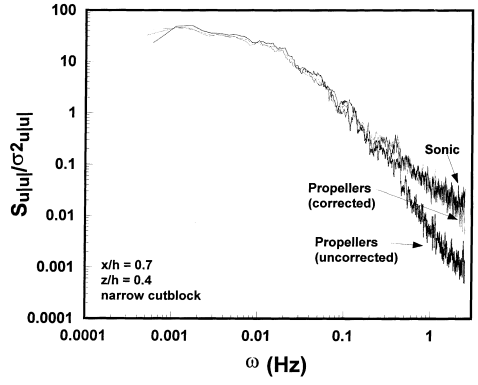

Fig. 11. Normalised power spectra of $u|u|$ ($S_{u|u|}$) versus frequency (ω) for a 30 min period during which there were simultaneous observations from a 3-D propeller and sonic anemometer. Also shown is the 'corrected' propeller spectrum, where the u|u| time series was corrected by applying a '−5/3 fall-off' to the propeller spectrum of u.

Acknowledgements

Funding for this work was provided by the Manning Diversified Forest Products Trust Fund. We are grateful for the help of Dr. Stan Navratil and Lorne Brace in initiating this work. A special thanks to Terry Thompson for his help with field work. The comments of an anonymous reviewer were appreciated.

Appendix A

Propeller anemometers errors

Propeller anemometers have poor high frequency response to wind fluctuations, and this results in errors in velocity statistics. A 3-D sonic anemometer (CSAT-3, Campbell Sci.) was temporarily co-located with a Gill UVW propeller anemometer at $x/\mathrm{h} = 0.6$ in the narrow cutblock ($z/\mathrm{h} = 0.4$), and the velocity statistics of $u|u|$ were compared (there was v interference with the propellers in these cases, and we did not compare $v|v|$ statistics). The propeller observations were corrected for cosine response using the algorithm of Horst (1972). We focused on two 30 min periods where $U > |V|$, and $\sigma_u > 0.5$ m. For simple wind force statistics, the agreement between the two anemometers was excellent. The magnitude of $\langle u|u|\rangle$ from the propeller exceeded that from the sonic by only 3%, while $\sigma_{u|u|}$ from the propeller exceeded that from the sonic by 5%. We therefore concluded that the propellers gave accurate estimates of $\langle u|u|\rangle$ and $\sigma_{u|u|}$ (and we believe accurate $v|v|$ statistics).

Though we were satisfied that the simple statistics of $u|u|$ and $v|v|$ from the propellers were accurate, we worried about errors in the power spectra $S_{u|u|}$. We were particularly concerned about underestimating $S_{u|u|}$ near the ω_n of our characteristic remnant spruce (0.4 Hz). A plot of $S_{u|u|}/\sigma_{u|u|}$ for one 30 min period, when both the sonic and propeller anemometers were operated simultaneously, shows that this underprediction did occur (Fig. 11). At $\omega \gtrsim 0.2$ Hz the propellers underestimated $S_{u|u|}$. At $\omega = 1$ Hz, $S_{u|u|}$ from the propellers was about one-tenth of the sonic value. We attempted to correct $S_{u|u|}$ (and $S_{v|v|}$) to give more accurate estimates of the three sway properties.

We began by correcting the velocity power spectra (S_u), extending the spectrum along the expected −5/3 'fall-off' at frequencies above 0.1 Hz (see Appendix in Flesch and Wilson, 1999). This correction is questionable within the forest, where vegetation elements may cause a 'short-circuit' of the normal energy cascade. We used the corrected S_u spectra and recreated the u time series for each measurement period (assuming the phase lag φ_u was without error – we had no theoretical basis to judge φ_u accuracy). From this 'corrected' time series of u, we recalculated the $u|u|$

series, and a 'corrected' $S_{u|u|}$. How well does this correction work? Fig. 11 shows that for one 30 min period, the corrected propeller $S_{u|u|}$ was in good agreement with that from the sonic. The other periods showed similar results. All the $u|u|$ and $v|v|$ series were corrected in this manner.

References

Blackburn, P., Petty, J.A., Miller, K.F., 1988. An assessment of the static and dynamic factors involved in windthrow. Forestry 61, 29–43.

Chatfield, C., 1984. The Analysis of Times Series, Chapman and Hall, London, 286 pp.

Flesch, T.K., Grant, R.H., 1991. The translation of turbulent wind energy to individual corn plant motion during senescence. Boundary-Layer Meteor. 55, 161–176.

Flesch, T.K., Wilson, J.D., 1993. Extreme value analysis of wind gusts in Alberta. Partnership Agreement in Forestry (PAR) Report 107, Nat. Resour. Can., Can. For. Serv., Northwest Reg., Edmonton, Alb., Canada.

Flesch, T.K., Wilson, J.D., 1999. Wind and remnant tree sway in forest cutblocks: I. Measured wind in experimental cutblocks, Agric. For. Meteorol. 93, 229–242.

Gardiner, B.A., 1994. Wind and wind forces in a plantation spruce forest. Boundary-Layer Meteorol. 67, 161–186.

Gardiner, B.A., 1995. The interactions of wind and tree movement in forest canopies, In: Coutts, Grace, (Eds.), Wind and Trees, Cambridge University Press, Cambridge, 485 pp.

Holbo, H.R., Corbett, T.C., Horton, P.J., 1980. Aerodynamic behavior of selected Douglas-fir. Agric. Meteorol. 21, 81–91.

Horst, T.W., 1972. A computer algorithm for correcting non-cosine response in the Gill anemometer, Pacific Northwest Laboratory Annual Report for 1971 to the USAEC Division of Biology and Medicine, vol. II: Physical Sciences, Part 1: Atmospheric Sciences, BNWL-1651–1. Battelle, Pacific Northwest Laboratories, Richland, WA.

Meirovitch, L., 1986. Elements of Vibration Analysis, McGraw-Hill, New York.

Mayer, H., 1987. Wind-induced tree sways. Trees 1, 195–206.

Milne, R., 1991. Dynamics of swaying *Picea sitchensis*. Tree-Physiol. 9, 383–399.

Oliver, H.R., Mayhead, G.J., 1974. Wind measurements in a pine forest during a destructive gale. Forestry 47, 185–195.

Stacey, G.R., Belcher, R.E., Wood, C.J., Gardiner, B.A., 1994. Wind flows and forces in a model spruce forest. Boundary-Layer Meteorol. 69, 311–334.

Thom, A.S., 1971. Momentum absorption by vegetation. Quart. J. Roy. Meteorol. Soc. 94, 414–428.

Wilson, J.D., Flesch, T.K., 1999. Wind and remnant tree sway in forest cutblocks, III: A wind flow model to diagnose spatial variation, Agric. For. Meteorol. 93, 259–282.

Wood, C.J., 1995. Understanding wind forces on trees, In: Coutts and Grace, (Eds.), Wind and Trees, Cambridge University Press, Cambridge, 485 pp.